International Conference on Applied Energy 2019
Aug 12-15, 2019, Västerås, Sweden
Paper ID: 0879

A Facile Synthesis Strategy of Ni@yolk-meso-SiO_2 for Catalytic Dry Reforming of Methane

Zi-Yian Lim [1,2], Xiaoxi Ma [1], Baiman Chen [2*]

1 School of Electric Power, South China University of Technology, Guangzhou 510640, China.

2 Guangdong Provincial Key Laboratory of Distributed Energy Systems, School of Chemical Engineering and Energy Technology, Dongguan University of Technology, Dongguan 523808, China.

ABSTRACT

This paper reports a synthesis strategy to develop Ni@yolk-meso-SiO_2 by adopting the leaching and re-deposition of silica in mild alkaline solution with CTAB as stabilizer. It was compared to Ni@SiO_2 core-shell catalyst and point out their difference in catalytic performance. The catalyst shows stable and near equilibrium conversion of methane and carbon dioxide for 50 hours. The increased in surface area and total pore volume contributed its high activity and stability.

Keywords: Dry reforming, Methane, Yolk-shell, leaching, re-deposition.

1. INTRODUCTION

Oxide-supported Nickel catalysts have become a hot research topic in recent years, and their preparations, properties and modifications have been intensively investigated[1]. Due to their high affinity in methane dissociation and reduction properties, Ni-based catalysts have been proposed to be promising candidates in hydrocarbon/CO_2 reforming and hydrogen production. However, Ni-based catalysts tend to sinter at high temperatures during pre-treatment and catalytic process[2]. Furthermore, carbon fouling in the catalyst will eventually lead to deactivation due to sintering of the Ni metal particles that dependent on the selection of supports[3], which is still primary challenges in industry.

Synthesizing core-shell structures has been considered as an efficient and promising strategy to prevent active metal nanoparticles from agglomeration[4]. The composites are designed to encapsulate active metal nanoparticles with permeable shells to obtain reactant gaseous exchange and isolation of active metal nanoparticles simultaneously. Typically, SiO_2[5], ZrO_2[6], and Al_2O_3[7] have been reported as the shell materials. Among them, SiO_2 was the most widely adopted due to its high thermal stability and controllable morphology. Most of the Ni@SiO_2 spheres were prepared via microemulsion methods to synthesize Ni particles and coat the Ni particles with SiO_2 respectively. The encapsulations of Ni particles by mesoporous SiO_2 shells with high surface area were still less highlighted, and the SiO_2 shells limiting the mass transfer during reaction. Li et al studied the varied thickness of SiO_2 shell will caused agglomeration when SiO_2 shell thickness is thin, while the SiO_2 shell is thick, mass transfer of the reactant's gas was limited[8]. Thus, an adequate SiO_2 thickness is preferable for the dry reforming of methane. Another group studied the effect of hydrolysis time of TEOS and showed that shorter hydrolysis time possesses highest specific surface area[9]. The shorter hydrolysis time sample (Ni@SiO_2-1h) exhibited excellent stability and low carbon depositions. However, the control of the thickness of the SiO_2 was found to be difficult. Recently, a Pd@SiO_2 core-shell nanocatalyst has been prepared via a sol-gel method for dry reforming methane and it exhibited high catalytic reaction and high coking resistance[10]. It was proposed that the removal of PVP and CTAB generate large numbers of mesopores in the SiO_2 shell, resulting in large surface area for Pd@SiO_2. Inspired by these studies, we focused on the preparation method of Ni@yolk-meso-SiO_2 for dry reforming methane.

In this paper, a mild leaching and re-deposition of silica was adopted to synthesize the Ni@yolk-meso-SiO_2. Firstly, a sub-50 nm Ni@SiO_2 nanoparticles were prepared by reverse microemulsion and calcined at 500 °C; secondly, the calcined Ni@SiO_2 nanoparticles were treated under mild alkaline solution with CTAB as stabilizer at 50 °C for 7 hours. The CTAB will direct the surface leaching of silica and act as template for re-deposition of silica; finally, the CTAB surfactants were removed by calcining the as-synthesized sample to produce Ni@yolk-meso-SiO_2.

2. EXPERIMENTAL SECTION

2.1 Catalyst synthesis

Selection and peer-review under responsibility of the scientific committee of the 11th Int. Conf. on Applied Energy (ICAE2019).

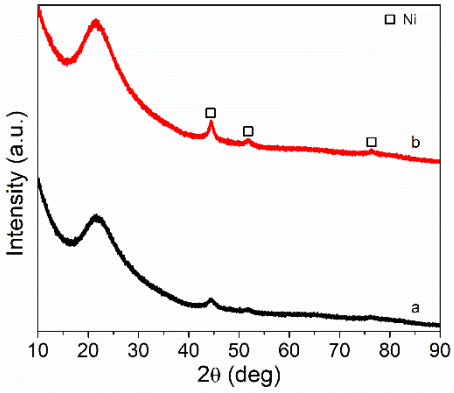

Fig 1. XRD patterns of Ni@SiO_2 (a) and Ni@yolk-meso-SiO_2 (b).

Synthesis of Ni@SiO_2. 3 mL of aqueous 0.25M $NiCl_2$ and 11.5 mL of Brij L4 (Sigma-Aldrich) were mixed with 40 mL of n-octane in a 250 mL 3-neck round bottom flask at 30 °C under N_2 atmosphere protection. The mixture was stirred for 10 minutes before 1 mL of 3.172 M ice-cold $NaBH_4$ solution was quickly dropped into the flask. Immediately, the clear solution would turn pitch black and bubbles were generated. After 5 minutes of N_2 purge, the flask was sealed. Next, the solution was stirred for 8 hours to form stable Ni colloids. The SiO_2 coating was achieved by subsequently adding 50 mL of n-octane, 2.4 mL Brij L4, 1.2 mL ammonia (26-28%), and 10 mL of TEOS into the solution. The solution was stirred continuously for 3 hours. After 3 hours, additional 2 mL of TEOS was added and stirred for another 5 hours. The Ni@SiO_2 colloids were obtained after centrifugation and washed with acetone and ethanol. The slurry was dried at 105 °C for 3 hours and calcined at 550 °C with 1.5 °C/min heating rate for 3 hours.

Synthesis of Ni@yolk-meso-SiO_2. 0.75 g of calcined Ni@SiO_2 powder were dispersed in 150 mL of deionized water by ultrasonication for 10 min. Then, following addition of 0.19 g of CTAB to the mixture and stirred under 50 °C for 15 min. The mixture was added 3.18g of Na_2CO_3 and react for 7 hours. The catalyst was collected by centrifugation and were washed with deionized water and ethanol several times. After drying at 105 °C for 3 hours, the powder was calcined at 550 °C for 3 hours at 1.5 °C/min heating rate. Subsequently, the obtained powder was reduced under 50% H_2/N_2 at 750 °C for 3 hours.

2.2 Catalyst Characterization

X-ray diffraction (XRD) spectra were collected on a D8 Rigaku 9000 powder diffractometer, equipped with Cu Kα radiation (λ = 1.5406 Å) in the 2θ range of 10°-90° at operation voltage of 45 kV and current of 200 mA. The specific surface area was determined by the BET method with N_2 adsorption-desorption at 77 K using a Micromeritics ASAP 2460. Prior to the measurements, the samples were degassed at 300 °C for 8 hours under vacuum. Transmission electron microscopy (TEM), model FEI Tecnai G2 F20 was used to study the morphology and microstructure of the catalyst. The specimens were prepared by dropping a trace amount of the sample dispersed in ethanol on a carbon-coated copper grid (300 mesh). ICP-MS (Inductively Coupled Plasma Mass Spectrometry) was performed on an Agilent 720 system to obtain each sample's Ni wt% content. After each test, the acid-digested sample was diluted with deionized water to 100 mL prior to the analyser. X-ray photoelectron spectroscopy (XPS) spectra were recorded on a Shimadzu Axis Ultradld spectroscope using a monochromatized Al Kα radiation source at room temperature and under a vacuum of 10^{-7} Pa (10^{-9} Torr). The starting angle of the photoelectron was set at 90°. The spectrum was calibrated with C 1s spectrum of 284.8 eV. Thermogravimetric analysis (TGA) was conducted using STA 449F3 (NETZSCH) equipment. The tested catalysts were preheated under a flow of nitrogen for 30 min. Then the samples were heated in air by raising the temperature from room temperature to 1000 °C at a rate of 10 °C min^{-1}. Raman spectra were collected using a WITec Alpha 300R (λ = 532 nm) and a CCD detector. The spectrum acquisition consisted of 3 accumulations for 45 s. The spectra were recorded at ambient temperature.

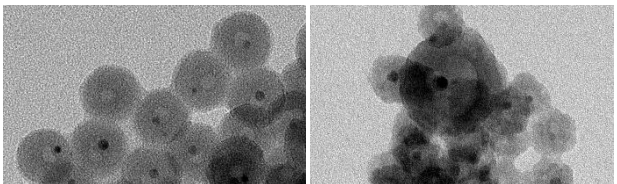

Figure 2. TEM images of Ni@SiO_2 (left) and Ni@yolk-meso-SiO_2 (right) catalysts.

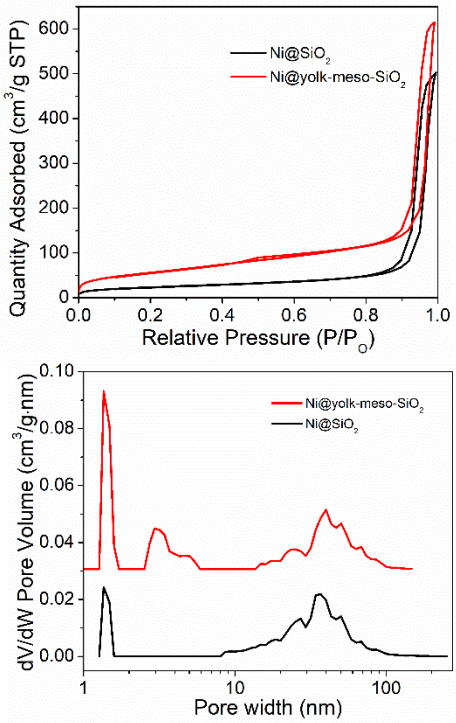

Figure 3. N_2-isotherm and pore size distribution of the catalysts.

2.3 Catalyst Evaluations

Table 1. Physical properties of Ni@SiO_2 and Ni@yolk-meso-SiO_2 catalysts.

Sample	Ni wt%	Ni particle size [a] (nm)	Specific surface area (m^2g^{-1})	Total pore volume (cm^3g^{-1})
Ni@SiO_2	2.18	5.8	84	0.75
Ni@yolk-meso-SiO_2	3.77	11.0	203	0.94

a Measure from TEM micrographs

Catalytic dry reforming of methane was studied in a fixed bed quartz reactor (15 mm ID) under atmospheric pressure. Typically, 100 mg of catalyst diluted with filled zirconia ceramic sand of 2 cm length was used. The quartz reactor loaded with catalyst was heated in an electric furnace and the temperature of the bed was controlled by a K-type thermocouple positioned at the center of the catalyst bed. Prior to the test, the catalyst was reduced in situ 750 °C with 50%H_2/N_2 mixture (40 mL min^{-1}) for 3 hours. A reaction mixture of N_2, CH_4 and CO_2 (ratio of 1:1:1) was fed using a gas hourly space velocity (GHSV) of 54000 mL g_{cat}^{-1} h^{-1}. The composition of the effluent gases was analysed by an on-line gas chromatography (Fuli 9790) equipped with a packed column (TDX-01) and a TCD detector. A cold trap was placed before the GC to remove moisture in the gas products.

2.4 Results and Discussion

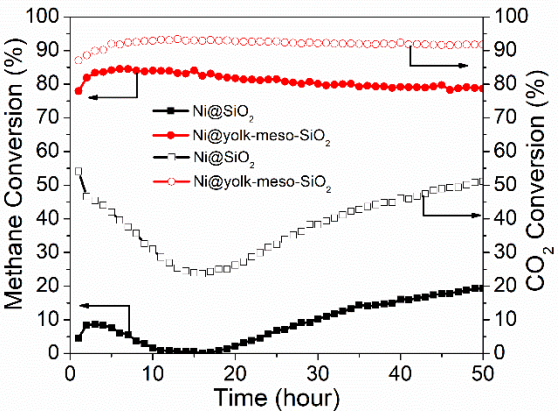

Figure 4. Catalytic performance of dry reforming of methane on Ni@SiO_2 and Ni@yolk-meso-SiO_2 catalysts. Conditions: 800 °C, GHSV = 54 000 mL$g_{cat}^{-1}h^{-1}$, N_2:CH_4:CO_2 = 1:1:1.

XRD patterns of the catalysts are shown in Fig. 1. Both catalysts showed the characteristic of amorphous SiO_2 and Ni metal. The peaks observed at 2θ = 44.5°, 51.8°, and 76.4° can be assigned to the (111), (200), (220) planes of Ni metal, respectively. The average crystallite size of Ni is shown in Table 1 and was determined using the Scherrer formula by the peak of Ni (111) reflection in the XRD patterns. The crystallite size was used to compared with the particle size results obtained from the TEM study. This would help to give insight if increasing the synthesis temperature would affect the crystallite size. From the observation of XRD, Ni@yolk-meso-

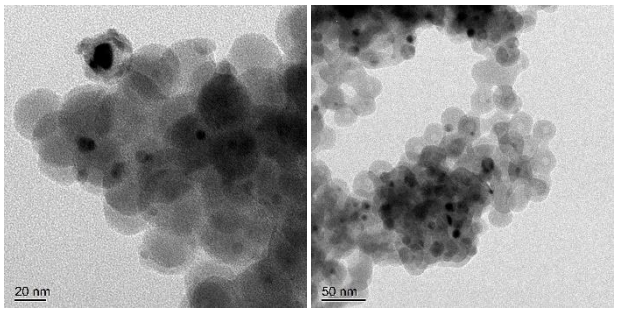

Figure 5. TEM images of tested Ni@SiO_2 (left) and Ni@yolk-meso-SiO_2 (right) catalysts.

SiO_2 has higher intensity of Ni (111) plane than Ni@SiO_2 catalyst and their crystallite size were 8.3 nm and 11.0 nm respectively. This indicated that the leaching and re-deposition of silica had cause Ni particles growth during synthesis of Ni@yolk-meso-SiO_2. Furthermore, from TEM analysis (Fig 2.) showed that Ni@SiO_2 has defined yolk-shell structure and small Ni particles were well dispersed in each SiO_2 nanosphere. While Ni@yolk-meso-SiO_2 had less defined yolk-shell structure, larger Ni particles that are not well dispersed in each SiO_2 nanosphere. Table 1 showed their respective measured Ni particle size from TEM. This suggested the leaching and re-deposition of silica inevitably caused Ni particle growth; however, the treatment did not cause significant changes on the morphology. It still retains the yolk-shell morphology and Ni particles are inside the SiO_2 nanospheres.

The N_2-isotherm graph showed that the catalysts have Type-IV isotherm characteristic (Fig. 3). The hysteresis loop changed from Type H3 to H2 after the mild alkaline treatment with CTAB. In addition, the adsorption capability increased significantly and mesopores were generated. This could be the CTAB act as the template for mesopore characteristic in SiO_2 shell after calcination while maintaining the morphology of yolk-shell structure. This can be also observed from the pore size distribution of the catalysts (Fig. 3). It showed that the both catalysts have micropores situated at approximately 1.4 nm, even so, Ni@yolk-meso-SiO_2 has higher amount of micropores compared to Ni@SiO_2. Furthermore, approximate 3.2 nm of mesopores exist in Ni@yolk-meso-SiO_2 which contributed in the total pore volume (Table 1). Thus, the treatment of mild alkaline solution with CTAB drastically changed the physisorption of Ni@SiO_2.

Table 2. XPS analysis of the relative mass concentration of Ni@SiO_2 and Ni@yolk-meso-SiO_2 catalysts before and after the dry reforming test.

Sample	Ni 2p wt%	Si 2p wt%	O 1s wt%
Ni@SiO_2-before	0.96	44.40	54.64
Ni@SiO_2-after	1.45	42.96	55.58
Ni@yolk-meso-SiO_2-before	1.45	44.22	54.33
Ni@yolk-meso-SiO_2-after	1.38	45.29	53.33

The catalytic dry reforming of methane of Ni@SiO_2 and Ni@yolk-meso-SiO_2 were studied at a GHSV of 54 000 mL$g_{cat}^{-1}h^{-1}$ with reaction mixture N_2:CH_4:CO_2 = 1:1:1 at 800 °C. and the

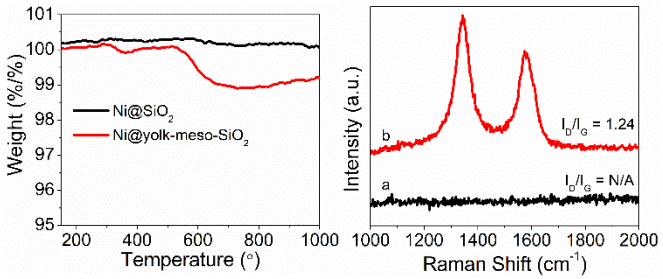

Figure 6. TGA and Raman analysis of tested Ni@SiO_2 and Ni@yolk-meso-SiO_2 catalysts.

results are shown in Figure 4. The methane conversion of Ni@SiO_2 showed poor or zero performance for the initial 15 hours of reaction and followed by increasing in conversion up to 19 % at 50 hours. In contrast, the Ni@yolk-meso-SiO_2 showed high methane conversion of 85% and stable at 79 % conversion for 50 hours. This is due to Ni@yolk-meso-SiO_2 has higher surface area, total pore volume, and mesopores characteristic. With such properties promote gaseous exchange and allowed higher methane conversion. Also, from the TEM observation (Fig. 5) of tested Ni@SiO_2 showed that some Ni particles escaped from the SiO_2 nanosphere. This phenomenon be clarified by XPS analysis (Table 2). Before the dry reforming test, the relative mass concentration of Ni was detected to be lower than 1%, but after test has increase to 1.45 %, while Ni@yolk-meso-SiO_2 did not change substantially. This indicated the Ni particles were moved onto the surface of SiO_2 nanospheres. From here, it can explain the initial drop in methane conversion and followed by increase in conversion for Ni@SiO_2.

Carbon deposition during dry reforming of methane is inevitable and causes the deactivation of catalysts. It was extensively studied that, Boudouard reaction and methane decomposition were the primary source of carbon fouling in catalysts. Therefore, thermogravimetric analysis (Fig. 6a) was conducted for the spent Ni@SiO_2 and Ni@yolk-meso-SiO_2, whereas negligible of carbon deposition can be observed for Ni@SiO_2. This is probably due to the thick SiO_2 shell that limit reactant gases permeate to the active Ni particles and low methane dissociation occurred, hence, negligible of carbon is deposited in Ni@SiO_2. For Ni@yolk-meso-SiO_2, it has trace amount of carbon deposited with approximately 1 % from TGA analysis. However, this degree of carbon deposition can be overlooked since it operated for 50 hours and still maintained high catalytic activity. Further, a Raman test (Fig. 6b) was conducted, suggesting the carbon deposited in Ni@yolk-meso-SiO_2 dominantly disordered carbon. It was observed that the spectra of D band and G band of carbon has the relative intensity ratio I_D/I_G more than 1. It implies that the carbon deposited in the catalyst could be easily removed by the reactant gas (CO_2) or re-treatment with H_2 for catalyst regeneration. It can be concluded that the Ni@yolk-meso-SiO_2 exhibit high thermal and high coking resistant for catalytic dry reforming of methane.

CONCLUSIONS

Ni@yolk-meso-SiO_2 was successfully synthesized via the treatment in mild alkaline solution with CTAB as a template and evaluated for dry reforming of methane. This study showed the differences in performance between a rigid Ni@SiO_2 and porous Ni@yolk-meso-SiO_2. It was found that the treated Ni@SiO_2 particles have greatly increase in surface area and pore volume. In addition, the Ni particles was maintained inside the SiO_2 nanosphere during the leaching and re-deposition of silica due to the CTAB stabilizing the morphology of the yolk-shell structure. The CTAB would be the template for mesopore characteristic in the SiO_2 shell. It is remarkable to develop such properties of the catalyst which is possible to be applied other core-shell nanoparticles.

ACKNOWLEDGEMENT

This work was supported by the DGUT-Postdoctoral Starting Funds (GC300501-24), The Science and Technology Innovation Service Program 2018 (code: 2018010), Engineering Research Center of None-food Biomass Efficient Pyrolysis and Utilization Technology of Guangdong Higher Education Institutes (2016GCZX009), and The National Natural Science Foundation of China (No. 51606042).

REFERENCE

[1] Z. Bian, S. Das, M.H. Wai, P. Hongmanorom, S. Kawi,ChemPhysChem, 18 (2017) 3117-3134.
[2] K.O. Christensen, D. Chen, R. Lødeng, A. Holmen,Applied Catalysis A: General, 314 (2006) 9-22.
[3] J. Sehested,Catalysis Today, 111 (2006) 103-110.
[4] Z. Li, Z. Wang, S. Kawi,ChemCatChem, 11 (2019) 202-224.
[5] J.C. Park, J.U. Bang, J. Lee, C.H. Ko, H. Song,Journal of Materials Chemistry, 20 (2010) 1239-1246.
[6] P.M. Arnal, M. Comotti, F. Schüth,Angewandte Chemie International Edition, 45 (2006) 8224-8227.
[7] X. Fang, Z. Liu, M.-F. Hsieh, M. Chen, P. Liu, C. Chen, N. Zheng,ACS Nano, 6 (2012) 4434-4444.
[8] Z. Li, L. Mo, Y. Kathiraser, S. Kawi,ACS Catalysis, 4 (2014) 1526-1536.
[9] F. Wang, B. Han, L. Zhang, L. Xu, H. Yu, W. Shi,Applied Catalysis B: Environmental, 235 (2018) 26-35.
[10] L. Yue, J. Li, C. Chen, X. Fu, Y. gong, X. Xia, J. Hou, C. Xiao, X. Chen, L. Zhao, G. Ran, H. Wang,Fuel, 218 (2018) 335-341.